DMD Fast Forward. Published on April 28, 2014 as doi: 10.1124/dmd.114.057430

TITLE PAGE

Identification of a functional homologue to the mammalian CYP3A4 in locusts

Line Rørbæk Olsen, Charlotte Gabel-Jensen, Peter Aadal Nielsen, Steen Honoré Hansen, and Lassina Badolo.

Department of Pharmacy, Faculty of Health and Medical Sciences, University of Copenhagen, DK-2100 Copenhagen, Denmark (LRO, CGJ, SHH)

Department of Discovery ADME, H. Lundbeck A/S, Ottiliavej 9, 2500 Valby, Denmark (LB)

EntomoPharm R&D, Medicon Village, S-223 81 Lund, Sweden (PAN)

DMD Fast Forward. Published on April 28, 2014 as DOI: 10.1124/dmd.114.057430
This article has not been copyedited and formatted. The final version may differ from this version.

RUNNING TITLE PAGE

Comparison of Terfenadine Metabolism in Locusts and HLM

Corresponding should be addressed to: Line Rørbæk Olsen; line.olsen@sund.ku.dk

Phone. +45 35336102

Department of Pharmacy, Faculty of Health and Medical Sciences, University of Copenhagen, DK-2100 Copenhagen, Denmark

Text pages: 30

Tables: 2

Figures: 9

References: 31

Abstract: 221

Introduction: 453

Discussion: 1276

Nonstandard abbreviations: AUC, area under curve; BBB, blood-brain barrier; CNS, central nervous system; HLM, human liver microsomes; HR-MS, high resolution mass spectrometry; Pgp, P-glycoprotein; UHPLC, ultra high performance liquid chromatography

Abstract

Insects have been proposed as a new tool in early drug development. It was recently demonstrated, that locusts have an efflux transporter localized in the brain barrier that is functionally similar to the mammalian P-glycoprotein (P-gp) efflux transporter. Two insect BBB models have been put forward, an *ex vivo* model and an *in vivo* model. In order to use the *in vivo* model it is necessary to fully characterize the locust as an entire organism with regards to metabolism pathways and excretion rate. In the present study, we have characterized the locust metabolism of terfenadine, a compound that in humans is specific to the cytochrome P450 enzyme 3A4. Using high resolution mass spectrometry (HR-MS) coupled to UHPLC we have detected metabolites identical to human metabolites of terfenadine. The formation of human metabolites in locusts was inhibited by ketoconazole, a mammalian P450 3A4 inhibitor, suggesting that the enzyme responsible for the human metabolite formation in locusts is functionally similar to human P450 3A4. Besides the human metabolites of terfenadine, additional metabolites were formed in locusts. These were tentatively identified as phosphate and glucose conjugates. In conclusion, locusts may not only be a model useful for determining BBB permeation, but possibly insects could be used in metabolism investigation. However, extensive characterization of the insect model is necessary in order to determine the applicability.

DMD Fast Forward. Published on April 28, 2014 as DOI: 10.1124/dmd.114.057430
This article has not been copyedited and formatted. The final version may differ from this version.

Introduction

Today, most new drugs that fail in the clinical phase do so due to lack of desired pharmacological activity or toxicity (Hughes et al., 2011). In the development of CNS drugs the blood brain barrier (BBB) creates additional challenges and therapeutic agents for the treatment of neurological disorders often fail in clinical trials due to inadequate BBB permeation (Alavijeh et al., 2005; Geldenhuys et al., 2012). *In vitro* methods for testing BBB penetration are either too simple, not integrating the complexity of the BBB, and therefore may lack important functions of the BBB (Naik and Cucullo, 2012). Preclinical *in vivo* models are very costly in terms of time and use of animals (rodents). Fast screening models for the BBB permeation are therefore very attractive.

Insects have been suggested as a novel model in drug discovery (Geldenhuys et al., 2012). It has been demonstrated, that locusts among other insects have an efflux transporter that is functionally similar to the mammalian P-glycoprotein (P-gp) efflux transporter (Nielsen et al., 2011).

Currently, two insect BBB models have been reported using locusts as model insects (Nielsen et al., 2011; Andersson et al., 2013). An *ex vivo* model has been developed and allows applying test items directly on entire brains isolated prior to testing. Beside this model, an *in vivo* model has also been developed where the test item is injected in the hemolymph and may need to pass the barriers of metabolism and excretion before reaching the brain. As such, the *in vivo* locust model may have more similarities with other *in vivo* models like rodent models. Also, the brain remains in its natural environment with no risk of impairing the barrier function.

Despite obvious anatomical differences, there are many physiological and biochemical similarities between insects and mammals. Essential systems such as protein synthesis and

DMD Fast Forward. Published on April 28, 2014 as DOI: 10.1124/dmd.114.057430
This article has not been copyedited and formatted. The final version may differ from this version.

cell metabolism are not significantly different between insects and mammals (Klowden, 2007). Mono-oxygenases like the cytochrome P450 enzymes are found in virtually all eukaryotic organisms including insects (Scott, 2008). This is of specific interest as some of the most important drug metabolizing enzymes in humans are the cytochrome P450 enzymes. Of mammalian P450 enzymes, the sub-families P450 1A1/2, 2B6, 2C9/19, 2D6, 2E1, and 3A4/5 are the main contributors, where P450 3A4 account for the metabolism of almost half of all marketed drugs (Guengerich, 2007).

Most literature on insect metabolic systems concerns insecticide detoxification mechanisms and resistance development (Smith, 1962; Wilkinson and Brattsten, 1972; Feyereisen, 1999; Scott and Wen, 2001). Furthermore, most research was conducted in the 1950's and 1960's where the analytical methods were limited, compared to the technologies available today.

In the present study, we have characterized the metabolism in locusts of the antihistaminic drug terfenadine, a specific human P450 3A4 substrate.

DMD Fast Forward. Published on April 28, 2014 as DOI: 10.1124/dmd.114.057430
This article has not been copyedited and formatted. The final version may differ from this version.

Materials and Methods

Solvents and reagents: All solvents used were at least of HPLC-grade. Methanol (MeOH) was purchased from BDH prolabo (VWR, Herlev, Denmark). Following reagents were purchased from Sigma-Aldrich (St Louis, MO): Female, pooled human liver microsomes (HLM), glucose-6-phosphate, glucose-6-phosphate dehydrogenase from Baker's yeast, $NADP^+$, formic acid, $MgCl_2 \cdot 6\ H_2O$, quinidine, α-naphtoflavone, sulfaphenazole, nootkatone, ketoconazole, and amitriptylin. The following were purchased from Merck (Darmstadt, Germany): $K_2HPO_4 \cdot 3H_2O$, KH_2PO_4, $ZnSO_4 \cdot 7\ H_2O$, and DMSO. Terfenadine was kindly provided by Neurosearch A/S (Ballerup, Denmark). Water for mobile phases and solutions were purified with a Millipore Direct-Q3 UV system (Billerica, MA, USA).

Animals: Male desert locusts, Schistocerca gregaria (L), were obtained from a commercial breeder (Petra Aqua, Prague, Czech Republique). The locusts were housed under crowded conditions at a 12 hour light/dark cycle at 25-35 °C. They had constant access to Chinese cabbage and dried wheat bran. Experiments were carried out on fed fifth instar locusts aged 3-5 weeks after final moult.

Locust experiments: Terfenadine, quinidine, sulfaphenazole, nootkatone, α-naphthoflavone, and ketoconazole were dissolved in DMSO and diluted with 0.1% lactic acid in milliQ water to the applied concentrations. Terfenadine was administered alone or in a co-solution with one of the following P450 in inhibitors: ketoconazole, quinidine, sulfaphenazole, nootkatone, or α-naphthoflavone. DMSO concentrations in all solutions used for injection were 7.5 % due to low solubility of some of the inhibitors. The locusts contain approximately 144 µL hemolymph/g (Lee, 1961) and had an average weight of 1.59 g (+/- 0.166, Mean and SD, n = 10) and thus the final DMSO concentration in hemolymph is expected to be < 2 %.

DMD Fast Forward. Published on April 28, 2014 as DOI: 10.1124/dmd.114.057430
This article has not been copyedited and formatted. The final version may differ from this version.

The locusts were injected with 40 µL of 500 µM terfenadine (with and without 2.5 mM inhibitor) between two terga and kept fixated at room temperature during the experiment. The effect of different P450 inhibitors were determined using a hemolymph sample 60 minutes post injection (n = 4). If significant inhibition of terfenadine metabolism was observed, time profile of metabolites formed were obtained from hemolymph samples over a time period of 2 hours. Hemolymph samples were taken from the locust at 1, 5, 10, 20, 30, 45, 60, and 120 minutes post administration. Samples were collected using an end-to-end micro pipette (10 µL) through a small hole, punctured in the soft tissue below the head. The collected hemolymph was added to 40 µL 2 % $ZnSO_4$ in 50 % MeOH (on ice) containing amitriptyline as internal standard. After 120 minutes, the locusts were euthanized by freezing. For detection of metabolites in feces, locusts were dosed with 40 µL 500 µM terfenadine (with or without 2.5 mM inhibitor) and left for 24 hours. Then, feces were collected and weighed and metabolites were extracted with 50 % MeOH containing internal standard by ultrasonication for 30 minutes.

All samples collected were stored at -18 °C prior to analyzing. After thawing, the hemolymph samples were centrifuged for 10 minutes at 15,000 x g at 5°C and the supernatants transferred to vials for analysis. The fecal extracts were filtered through 0.45 µm Millex-HV syringe filters (Millipore, Bedford, MA) and analyzed. Hemolymph and feces from non-treated locusts were used as controls.

HLM incubation method: HLM (0.5 mg/mL) were pre-incubated at 37 °C for 5 minutes in 100 mM potassium phosphate buffer pH 7.4 with 3.3 mM $MgCl_2$, 0.4 U/mL glucose-6-phosphate dehydrogenase, 3.3 mM glucose-6-phosphate, and 1.2 mM $NADP^+$. After pre-incubation, terfenadine was added (final concentration 4 µM). Samples (20 µL) were taken out at the same timepoints as for the locust experiments and the reaction was quenched using

DMD Fast Forward. Published on April 28, 2014 as DOI: 10.1124/dmd.114.057430
This article has not been copyedited and formatted. The final version may differ from this version.

80 µL 2 % $ZnSO_4$ in 50 % MeOH, 3% formic acid (on ice). The samples were stored at -18 °C.

After thawing, the samples were centrifuged for 10 minutes at 15,000 x *g* at 5°C and the supernatants analysed with LC-MS.

In order to determine pharmacokinetic parameters (K_m) in locusts 5 different terfenadine concentrations were used (250 µM, 500 µM, 1000 µM, 1500 µM, and 2500 µM). The concentration of DMSO was kept at 2.5 % (less than 0.2 % in hemolymph). Fourty µL was injected and after 1 minute 20 µL of hemolymph was drawn from the locusts and added to 80 µL 2 % $ZnSO_4$ in 50 % MeOH containing internal standard. The samples were prepared in a Sirocco 96-well plate for protein precipitation (Waters, Milford, MA). The plate was centrifuged at 2000 x *g* for 4 minutes and the filtrate was collected and analyzed.

UHPLC-MS method: The chromatographic separation was performed on a Phenomenex Kinetex C_{18} (50 x 2.1 mm) column with 1.7 µm particles on a Dionex Ultimate 3000 RS UHPLC-system coupled to a high resolution MS instrument (Q Exactive Orbitrap with a HESI-II interface from ThermoFinnigan (San Jose, CA)). Separation was performed with gradient elution using 0.1 % formic acid in MilliQ water as mobile phase A and MeOH with 0.1 % formic acid as mobile phase B with a flow rate of 0.4 mL/min. The mobile phase B was kept at 5 % for 0.2 minutes followed by a linear gradient of 5-90 % B over 5 minutes, 90 % B for 1 minute followed by re-equilibration for 2 minutes. The column compartment was set to 30 °C and the samples were kept at 8 °C.

Detection of metabolites were performed in positive ionization mode using data-dependent MS^2 (dd-MS^2) on the top 5 most abundant ions in each scan with an dynamic exclusion of 5 sec. Quantification of terfenadine was performed in targeted MS^2 (tMS^2). The lock mass used (214.0896 *m/z*), originate from a plasticizer, n-butyl benzenesulfonamide. MS settings were as

shown in Table 1. Spray voltage was set to 3.3 kV, capillary temperature 350 °C, sheath gas 30 arbitrary units, auxiliary gas 10 arbitrary units, probe heater 250 °C and S-lens RF level 50. Thermo Scientific™ Mass Frontier 7.0 Spectral Interpretation Software was used for identification of metabolites.

For statistic evaluation a Student's t-test was used.

Results

HLM metabolites: To investigate whether metabolites obtained in the locust were similar to those obtained in humans, HLM was incubated with the test compound and the metabolites obtained here were used as reference compounds in comparison to locust metabolites. The phase I metabolites most frequently reported in the literature are shown in Figure 1 and were all detected in HLM and confirmed by accurate mass and fragmentation patterns (Jurima-Romet et al., 1994; Ling et al., 1995; Rodrigues et al., 1995).

Observed fragmentation pattern of terfenadine and metabolites are given in Table 2. Other metabolites and/or intermediates (M2, M7 and M8) were also identified in HLM. M1, M5, and M6 were identified as azacyclonol, terfenadine alcohol, and terfenadine acid, respectively and the structures are shown in Figure 1.

Substrate specificity in locust and mammals: To determine whether there is an enzyme in locusts with same substrate specificity as found in mammals, terfenadine was administered by intra-hemolymphic injection alone or along with each of five inhibitors known to inhibit different P450 enzymes (given in parenthesis) involved in drug metabolism; α-naphthoflavone (1A2), sulfaphenazole (2C9), nootkatone (2C19), quinidine (2D6), and ketoconazole (3A4). The results are shown in Figure 2. Only co-administration with ketoconazole resulted in a significant inhibition of formation of metabolites in locusts. The terfenadine dose given to the locusts corresponds to the weight adjusted daily oral dose in humans (120 mg ≈ 2 mg/kg) but dosed directly in the hemolymph.

DMD Fast Forward. Published on April 28, 2014 as DOI: 10.1124/dmd.114.057430
This article has not been copyedited and formatted. The final version may differ from this version.

Elimination of terfenadine from locust hemolymph was followed over time (Figure 3) and the area under curve (AUC) with and without co-administration of ketoconazole was calculated. As can be seen in Figure 3B, the AUC is significantly (1.7 fold) larger when ketoconazole is co-administered.

Detection of P450 metabolites in locusts: Metabolites were detected in locust hemolymph and feces with fragmentation pattern and retention times identical to metabolites identified in HLM incubations. The metabolites were not quantified; however, the relative amounts of the different metabolites were different in hemolymph and feces. Thus, M1 and M6 was the most abundant in hemolymph whereas M5 was more abundant in feces. M2, M3, M4, and M7 were only identified in feces. M3, M4, M9, M10, M11 and M12 were detected only in locusts.

M1, M5, M6, and M8 were all found in HLM incubations and in locust hemolymph as well as locust feces. M1, M6, and M8 increased over time when no inhibitor was co-administered as can be seen in Figure 4. In locust hemolymph M5 increased rapidly in the first 5 minutes and then decreased over time. This was also seen in HLM incubations, although, in the latter, the decrease started after 20 minutes. The formation of all four metabolites was inhibited almost completely by co-administration of ketoconazole.

Detection of non-P450 metabolites: Non-P450 metabolites were identified based on similarities in fragmentation pattern as seen in Table 2. Besides the 6 metabolites identified in HLM incubations, additional 6 metabolites were detected in locusts. Only four of these metabolites were detected in hemolymph in sufficient concentrations to be measured over time (Figure 5).

The excreted amount of unchanged terfenadine was not significantly different with and without co-administration of ketoconazole, but ranging from 3-30 % of the administered dose (data not shown). The exrection of only one metabolite was significantly increased when

DMD Fast Forward. Published on April 28, 2014 as DOI: 10.1124/dmd.114.057430
This article has not been copyedited and formatted. The final version may differ from this version.

ketoconazole was co-administered (M10). The formation of M12 appears to be inhibited by ketoconazole, however, the excreted amount of this metabolite was not significantly different (Figure 5 and Figure 6). The rest of the metabolites were inhibited (M7, M8, M9, and M11) or not affected (M3). M2 and M4 were also significantly inhibited by ketaconazole, however, the response of these metabolites were very low compared to the rest of the metabolites and therefore not included in the figures.

Metabolite identification:

A spectrum of M3 (*m/z* 650) is shown in Figure 7. Fragmentation of M3 is almost identical to the fragmentation of M5 suggesting that M3 is a conjugate of M5 ($\Delta m/z$ = 162). M3 was identified in locust feces and the amount excreted was not significantly changed when ketoconazole was co-administered. In hemolymph the concentration was too low to be followed over time suggesting that the excretion rate for this metabolite is high or that M3 is further metabolized.

As mentioned, the different metabolites were not quantified, however, based on the MS response M9 with an accurate mass of 568.281 was the most abundant metabolite found in locust feces and hemolymph. As seen in Figure 8, the fragmentation pattern resembles the fragmentation for terfenadine alcohol (M5). The fragment of 73 is missing and an additional fragment of 99 can be seen. In Figure 5 and Figure 6 it appears that the formation of M9 is significantly inhibited by ketoconazole.

M10 was identified as a direct conjugate of terfenadine without any prior phase I modification. According to Table 2, the mass of M10 corresponds to the *m/z* of terfenadine + 162. The fragmentation pattern for fragments with *m/z* < 472 was identical to terfenadine. In Figure 5 it can be seen that the formation rate of M10 was not affected by ketoconazole in the first 20 minutes post injection. From 20 minutes the amount of M10 increased significantly

DMD Fast Forward. Published on April 28, 2014 as DOI: 10.1124/dmd.114.057430
This article has not been copyedited and formatted. The final version may differ from this version.

compared to the amount in locusts only receiving terfenadine. The amount of excreted M10 was increased in locusts co-administered with ketoconazole.

M11 share some of the fragments seen for M7 and is expected to be a conjugate of M7. Fragmentation pattern were not similar regarding fragments with *m/z* <450. As can be seen in Figure 5 and Figure 6, formation of M11 is inhibited by ketoconazole.

M12 is expected to be a direct conjugate of terfenadine. The fragment of 472 (*m/z* of terfenadine) is missing in the MS^2 spectrum of M12 and only one water molecule is lost. Furthermore a fragment of 98.99 was observed. The formation of this metabolite in hemolymph was initially inhibited by ketoconazole (Figure 5). No significant difference could be shown for the amount excreted in feces when the locusts have been given ketoconazole (Figure 6).

Metabolite ID

Phase I metabolites: The fragmentation patterns of M1, M5, and M6 are described in the literature and these are consistent with the observed fragmentation pattern (Rodrigues et al., 1995). The fragmentation pattern of terfenadine has a characteristic loss of two consecutive water molecules from the parent mass and the *tert*-butyl group results in a fragment with *m/z* of 57. The fragmentation patterns of M5 and M6 show that the parent masses have shifted but there is still consecutive loss of two water molecules. The primary alcohol on M5 is too stable to result in a loss of water. The *tert*-butyl fragment of *m/z* 57 has shifted according to the metabolic modification, thus confirming where oxidation has taken place. Full structural elucidation by NMR of metabolites was not attempted and authentic standards were not available. Instead, fragmentation patterns and accurate mass was used for identification.

The MS responses of M2, M7, and M8 were minor and expected to be intermediates as reported by Jurima-Romet et al. (Jurima-Romet et al., 1994). M2 appears to be a double

hydroxylated metabolite. Both hydroxylations occur on the *tert*-butyl group as a fragment of 89.060 (57+16+16) was identified. The exact mass of M7 corresponds to an aldehyde and M8 to an acid-ketone metabolite. M4 has the same accurate mass as M2 but was only detected in locuts feces. Like M2 the fragementation pattern suggests that this metabolites could be a double hydroxylated compond, however, the fragmentation pattern was sligtly different compared to M2 (Table 2).

Phase II metabolites (locusts only):

Glucosylation: The metabolites M3 and M10 were only formed in locusts and was tentatively identified as glucosides of M5 and terfenadine, respectively. Δ*m/z* of both metabolites were 162 compared to M5 and terfenadine which corresponds to glucoside conjugates. The mass accuracy was better than 0.1 ppm. The glucose conjugation site of M10 could the amine or one of the secundary alcohols. Although highly speculative, it could be suggested that the glucosylation occur on the latter as there is only a single loss of water from M10 (634→616). The fragmentation pattern of M10 was identical to the fragmentation pattern of terfenadine for $m/z < 472$.

Regarding M3 it can be seen in Figure 7 that there are a consequtive loss of two water molecules (650→632→614), suggesting, that the glucose is conjugated to the nitrogen or the primary alcohol. The fragment with *m/z* 73 is formed confirming that the hydroxylation has occurred on the *tert*-butyl group of terfenadine.

Phosphorylation: M9, M11, and M12 were tentatively identified as a phosphate ester of terfenadine alcohol, M7, and terfenadine, respectively. The mass accuracy better than 0.5 ppm. Two consecutive water molecules are readily lost from M9, indicating that the phosphate ester is conjugated to the primary alcohol of M5 (Figure 8). The fragment of 434 ($M5 - 3H_2O$) is not seen in the MS/MS spectrum of terfenadine alcohol (M5). The fragment

is however seen in the spectrum of M9 suggesting that the phosphate group is more readily lost by fragmentation. Also, the fragment at *m/z* 73 indicating a hydroxylation on the *tert*-butyl group is also missing, indicating that the entire phosphate group is lost. The same pattern was observed for M12 where the fragment of 472 (*m/z* of terfenadine) is missing in the MS/MS spectrum of M12. Only one water molecule is lost suggesting that the phosphate forms an ester with one of the existing hydroxyl groups in the molecule. In the MS/MS spectra of all the phosphorylated metabolites a fragment of 98.99 could be seen. This fragment is thought to originate from protonated phosphate ($H_4PO_4^+$).

A proposed metabolism pathway of terfenadine in locusts can be seen in Figure 9.

Pharmacokinetic parameters

Due to extensive phase II metabolism of both parent and phase I metabolites a measure of the initial formation rate had to be done within one minute. At this time point substantial inter-individual variation was observed. Hence, estimation of pharmacokinetic parameters was not successful.

Discussion

Human phase I metabolites of terfenadine were produced in HLM and used as references to identify and characterize the metabolites in locusts. Metabolites identical to the metabolites detected in HLM incubations of terfenadine (M1, M2, M5, M6, M7, and M8) were identified in locust hemolymph and feces after administration of the drug. In humans, terfenadine is metabolized almost exclusively by P450 3A4 into the metabolites shown in Figure 1. Human data have shown increase in terfenadine AUC, after multiple dosing, ranging from 16 to 73 times when P450 3A4 is inhibited by ketoconazole (Honig et al., 1993), however, unchanged terfenadine is normally undetectable in plasma due to extensive first pass metabolism (Jurima-Romet et al., 1994). In *in vitro* assays using cryopreserved human hepatocytes ketoconazole provides almost complete inhibition of terfenadine metabolism (Shibata et al., 2008). In HLM the response of Azacyclonol (M1) increased in response over time in both HLM incubations and locust hemolymph. Terfenadine alcohol (M5) rose in the first 20 min and then declined, indicating, that this metabolite is further converted. The same was seen in locust hemolymph, only the decline started after 5 minutes. Terfenadine acid (M6) and M8 increased after a short lagtime in both HLM incubations and locust hemolymph, suggesting that M5 (terfenadine alcohol) was further converted into these metabolites. *In vivo* Km-values for the formation of phase I metabolites are not reported as unchanged terfenadine usually is undetectable in plasma when given in therapeutic doses (Jurima-Romet et al., 1994). *In vitro* data obtained using human liver microsomes resulted in K_m value for azacyclonol between 0.82 µM and 11 µM. The K_m values for hydroxy-terfenadine formation in human liver microsomes was ranging between 1.8 µM and 18 µM (Raeissi et al., 1997; Jurima-Romet et al., 1998).

DMD Fast Forward. Published on April 28, 2014 as DOI: 10.1124/dmd.114.057430
This article has not been copyedited and formatted. The final version may differ from this version.

Because no *in vivo* data is available for comparison and because the *in vitro* data varies considerably no further attempt to establish kinetic parameters for the metabolite formation was performed.

When locusts were exposed to a single dose of terfenadine combined with different P450 enzyme inhibitors, it was only ketoconazole (inhibitor of P450 3A4) that inhibited the formation of the mammalian metabolites, indicating that the formation of these metabolites in locusts is catalyzed by an enzyme functionally related to mammalian P450 3A4. As can be seen in Figure 3B, the AUC is significantly (1.7 fold) larger when ketoconazole is co-administered indicating that the elimination of terfenadine is inhibited. The excreted amount of terfenadine is not changed and compared to the inhibition observed in humans, the increase in AUC in the locusts is moderate, indicating that the metabolism of terfenadine may not be limited to a single enzyme and/or the enzyme(s) are not fully inhibited by ketoconazole. Based on the almost complete inhibition of formation of M1, M5, M6, and M8 in locusts (Figure 4), it seems likely that alternative metabolism pathways take part in terfenadine metabolism.

M3 and M10 were tentatively identified as glucose conjugates of terfenadine alcohol (M5) and terfenadine, respectively. In hemolymph the concentration of M3 was too low to be followed over time suggesting that the excretion rate is high for this metabolite. M10 increased significantly after 20 minutes from injection time compared to the amount in locusts only receiving terfenadine. The excreted amount of M3 was not significantly inhibited by ketoconazole even though the formation of M5 was significantly inhibited. M10 was increased in the presence of the P450 3A4 inhibitor. This is in agreement with the findings that other metabolism pathways are inhibited and thus, more terfenadine was available for glycosylation. However, the excreted amount of glucoside metabolites may be misleading due to glycosidase activity in the intestine (Kikal and Smith, 1959).

Previously, conjugates with amino acids, glucose, phosphate, and sulphate have been reported in insects (Myers and Smith, 1954; Smith, 1955; Smith, 1962; Cohen and Smith, 1964; Ngah and Smith, 1983). Glycosylation is mentioned a number of times in the literature as a detoxification mechanism in insects. Glycosylation can conjugate to amines, hydroxyl-, and carboxy-groups (Smith, 1968) and has been suggested to be analogue to mammalian glucuronidation (Smith, 1962). Although glucuronic acid conjugates have been reported in insects (Terriere et al., 1961) it has later been questioned in the literature (Lowenstein, 1968). Due to inadequate identification tools available in the 1950's and 1960's, metabolites may wrongfully have been identified as glucuronic acid conjugates.

It has been tested whether terfenadine and other tertiary amines could be metabolized into N-glucuronides (Luo et al., 1991). The study was conducted on healthy volunteers and for eight of the nine compounds tested glucuronides were detected in the urine. Terfenadine was the only compound of the nine tertiary amines tested that was not metabolized by the glucuronidation pathway. Glucoside formation has been reported in humans although the detoxification mechanism generally is considered to be characteristic in invertebrates and other lower organisms (Gessner et al., 1973). Based on the results in our study, regarding substrate specificity, glucuronidation in mammals does not appear to be an analogue to glycosylation in insects as no glucuronides of terfenadine have been reported. However, the two detoxification mechanisms are probably evolutionary related (Smith, 1968).

Phosphate and sulphate metabolites have been reported in insects (Smith, 1955; Ngah and Smith, 1983). Phosphate and sulphate conjugates of the same compound differ in mass by only 10 mmu. With accurate mass techniques we were able to distinguish between these two adducts. Thus, M9, M11, and M12 were tentatively identified as phosphate conjugates of M5 (terfenadine alcohol) M7, and terfenadine, respectively. Assuming the MS response of terfenadine and the metabolites are somewhat similar, M9 was the most abundant metabolite

found in locust feces and hemolymph (Figure 5 and Figure 6). In Figure 5 and Figure 6 it appears that the formation of M9 and M11 are significantly inhibited by ketoconazole, possibly due to inhibition of the oxidation step.

The structure of M7 was not confirmed by NMR and it is possible, that the carbonyl consists of a ketone rather than an aldehyde which is shown in Figure 9.

The formation of M12 in hemolymph was initially inhibited by ketoconazole even though P450 is not expected to be involved and no hydroxylation is required (Figure 5). However, the amount excreted in feces was not significantly different when the locusts have been given ketoconazole (Figure 6). Looking at Figure 5 it appears that there is a large increase in the amount M12 between 60 and 120 minutes post injection when ketoconazole is co-administered.

No sulphate metabolites of terfenadine were identified. Based on the present results, conjugation with phosphate and glucose seems to be major phase II detoxification pathways in locusts. These metabolites are qualitatively different from mammalian metabolism pathways and appear to some extent take over from P450 enzymes when these enzymes are inhibited.

Although many insecticides such as dimethoate have been developed due to the formation of toxic metabolites in insects but not in mammals (Smith, 1968), the phase I metabolism of terfenadine in locusts resembles the mammalian phase I metabolism. It is therefore possible, that the insect model could be used in phase I metabolism investigations and not only be useful for determining BBB permeation. The locusts may also be used in generating human relevant metabolites for further identification. However, extensive characterization of the insect models is necessary in order to determine the applicability. Inclusion of insect experiments in early preclinical drug development could possibly reduce costs as fewer

DMD Fast Forward. Published on April 28, 2014 as DOI: 10.1124/dmd.114.057430
This article has not been copyedited and formatted. The final version may differ from this version.

"poor" candidates would proceed to *in vivo* experiments in mammals. In the present study we have shown, that locusts may have an enzyme with a functionality similar to mammalian P450 3A4; an important enzyme involved in the human metabolism of almost half the marketed drugs (Guengerich, 2007).

Authorship Contribution

Participated in research design: Olsen, Hansen, Badolo, Gabel-Jensen

Conducting experiment: Olsen

Contributed new reagents or analytical tools: Hansen

Performed data analysis: Olsen, Hansen, Badolo

Wrote or contributed to the writing of the manuscript: Olsen, Hansen, Badolo, Gabel-Jensen, Nielsen

References

Alavijeh M, Chishty M, Qaiser M, and Palmer A (2005) Drug metabolism and pharmacokinetics, the blood-brain barrier, and central nervous system drug discovery. *NeuroRx* **2:**554-571.

Andersson O, Hansen SH, Hellman K, Olsen LR, Andersson G, Badolo L, Svenstrup N, and Nielsen PA (2013) The grasshopper: a novel model for assessing vertebrate brain uptake. *J Pharmacol Exp Ther* **346:**211-218.

Cohen AJ and Smith JN (1964) COMPARATIVE DETOXICATION .9. METABOLISM OF SOME HALOGENATED COMPOUNDS BY CONJUGATION WITH GLUTATHIONE IN LOCUST. *Biochem J* **90:**449-&.

Feyereisen R (1999) Insect P450 enzymes. *Annu Rev Entomol* **44:**507-533.

Geldenhuys WJ, Allen DD, and Bloomquist JR (2012) Novel models for assessing blood-brain barrier drug permeation. *Expert Opin Drug Metab Toxicol* **8:**647-653.

Gessner T, Jacknowi.A, and Vollmer CA (1973) Studies of Mammalian Glucoside Conjugation. *Biochem J* **132:**249-258.

Guengerich FP (2007) Cytochrome P450 and Chemical Toxicology. *Chem Res Toxicol* **21:**70-83.

Honig PK, Wortham DC, Zamani K, Conner DP, Mullin JC, and Cantilena LR (1993) Terfenadine-ketoconazole interaction: Pharmacokinetic and electrocardiographic consequences. *JAMA* **269:**1513-1518.

Hughes JP, Rees S, Kalindjian SB, and Philpott KL (2011) Principles of early drug discovery. *Brit J Pharmacol* **162:**1239-1249.

Jurima-Romet M, Crawford K, Cyr T, and Inaba T (1994) Terfenadine metabolism in human liver. In vitro inhibition by macrolide antibiotics and azole antifungals. *Drug Metab Dispos* **22:**849-857.

Jurima-Romet M, Wright M, and Neigh S (1998) Terfenadine-antidepressant interactions: an in vitro inhibition study using human liver microsomes. *Br J Clin Pharmacol* **45:**318-321.

Kikal T and Smith JN (1959) Comparative detoxication. 6. The metabolism of 6-amino-4-nitro-o-cresol and 4:6-dinitro-o-cresol in locusts. *Biochem J* **71:**48-54.

Klowden MJ (2007) *Physiological systems in insects*. Elsevier, Amsterdam.

Lee RM (1961) The variation of blood volume with age in the desert locust (Schistocerca gregaria Forsk.). *J Insect Physiol* **6:**36-51.

Ling KH, Leeson GA, Burmaster SD, Hook RH, Reith MK, and Cheng LK (1995) Metabolism of terfenadine associated with CYP3A(4) activity in human hepatic microsomes. *Drug Metab Dispos* **23:**631-636.

Lowenstein O (1968) Advances in Comparative Physiology and Biochemistry V3, Elsevier Science, Burlington.

Luo H, Hawes EM, McKay G, Korchinski ED, and Midha KK (1991) N(+)-glucuronidation of aliphatic tertiary amines, a general phenomenon in the metabolism of H1-antihistamines in humans. *Xenobiotica* **21:**1281-1288.

Myers CM and Smith JN (1954) Comparative Detoxication .2. Glucoside Formation from Phenols in Locusts. *Biochem J* **56:**498-503.

Naik P and Cucullo L (2012) In vitro blood–brain barrier models: Current and perspective technologies. *J Pharm Sci* **101:**1337-1354.

Ngah WZ and Smith JN (1983) Acidic conjugate of phenols in insects; glucoside phosphate and glucoside sulphate derivatives. *Xenobiotica* **13:**383-389.

Nielsen PA, Andersson O, Hansen SH, Simonsen KB, and Andersson G (2011) Models for predicting blood-brain barrier permeation. *Drug Discov Today* **16:**472-475.

Raeissi SD, Guo Z, Dobson GL, Artursson P, and Hidalgo IJ (1997) Comparison of CYP3A activities in a subclone of Caco-2 cells (TC7) and human intestine. *Pharm Res* **14:**1019-1025.

Rodrigues AD, Mulford DJ, Lee RD, Surber BW, Kukulka MJ, Ferrero JL, Thomas SB, Shet MS, and Estabrook RW (1995) In vitro metabolism of terfenadine by a purified recombinant fusion protein containing cytochrome P4503A4 and NADPH-P450 reductase. Comparison to human liver microsomes and precision-cut liver tissue slices. *Drug Metab Dispos* **23:**765-775.

Scott JG (2008) Insect cytochrome P450s: thinking beyond detoxification. *Recent Advances in Insect Physiology, Toxicology and Molecular Biology***:**117-124.

Scott JG and Wen ZM (2001) Cytochromes P450 of insects: the tip of the iceberg. *Pest Manag Sci* **57:**958-967.

Shibata Y, Takahashi H, Chiba M, and Ishii Y (2008) A Novel Approach to the Prediction of Drug-Drug Interactions in Humans Based on the Serum Incubation Method. *Drug Metab Pharmacokinet* **23:**328-339.

Smith JN (1955) Comparative detoxication. 4. Ethereal sulphate and glucoside conjugations in insects. *Biochem J* **60:**436-442.

Smith JN (1962) Detoxication Mechanisms. *Annu Rev Entomol* **7:**465-&.

Smith JN (1968) The comparative metabolism of xenobiotics. *Adv Comp Physiol Biochem* **3:**173-232.

Terriere LC, Roubal WT, and Boose RB (1961) Metabolism of Naphthalene and 1-Naphthol by Houseflies and Rats. *Biochem J* **79:**620-&.

Wilkinson CF and Brattsten LB (1972) Micrsomal Drug-metabolizing Enzymes in Insects.

Drug Metab Rev **1:**153-227.

DMD Fast Forward. Published on April 28, 2014 as DOI: 10.1124/dmd.114.057430
This article has not been copyedited and formatted. The final version may differ from this version.

FOOTNOTES

This work was supported by The Danish National Advanced Technology Foundation [Grant 023-2011-3].

Figure Legends

Figure 1: Structures of terfenadine and known metabolites formed in mammals by P450 3A4 (Jurima-Romet et al., 1994; Ling et al., 1995; Rodrigues et al., 1995).

Figure 2: Response of terfenadine and known mammalian metabolites after administration of terfenadine to locusts with and without co-administration of inhibitors. Mean and SEM, n = 4.

Figure 3: Elimination of terfenadine from hemolymph (A) and calculated AUC's (B). Results with (▲) and without (○) the inhibitor ketoconazole. Mean and SEM, n = 6.

Figure 4: Major metabolites identical to HLM metabolites identified in locust hemolymph over time. With (▲) and without (○) inhibitor. Mean and SEM, n = 6.

Figure 5: Major non-P450 metabolites identified in locust hemolypmh over time. With (▲) and without (○) inhibitor. Mean and SEM, n = 6.

Figure 6: MS response of terfenadine and the most abundant metabolites identified in feces collected from locuts 24 hours after injection (with and without co-administration of inhibitor). Left shows the metabolites significantly inhibited by co-administration of ketoconazole. Right is shown the metabolites unaffected or increased. Four locusts pr. cage. Mean and SEM, n = 3.

Figure 7: Fragmentation pattern of M3 (top) with parent mass of 650.369 and M5 (bottom) with parent mass of 488.316.

Figure 8: MS/MS spectrum of M9 with parent mass of 568.281 (top) and M5 with parent mass 488.315 (bottom).

Figure 9: Proposed metabolism pathways and structures of locust metabolites.

DMD Fast Forward. Published on April 28, 2014 as DOI: 10.1124/dmd.114.057430
This article has not been copyedited and formatted. The final version may differ from this version.

Tables

Table 1: MS settings for identification of metabolites.

	Full scan	dd-MS^2	tMS^2
Resolution	70,000	17,500	17,500
AGC target	3e6	1e5	2e5
Maximum injection time	100 ms	50 ms	100 ms
Scan range	200-750	-	-
Isolation window	2.0 *m/z*		1 *m/z*
NCE	-	35	35
Underfill ratio		0.1 %	

DMD Fast Forward. Published on April 28, 2014 as DOI: 10.1124/dmd.114.057430
This article has not been copyedited and formatted. The final version may differ from this version.

Table 2: Metabolites identified in locust feces and HLM.

Compound	RT (min) Locusts hemolymph and/or feces	RT (min) HLM	Parent *m/z*	Major fragment *m/z*	Other fragment *m/z*
M1 (Azacyclonol)	3.45	3.47	268.170	250.159	167.085
M2	3.79	3.81	504.311	468.289	486.299, 262.158, 89.060
M3	4.15	N.F.	650.369	452.294	632.357, 614.345, 470.305, 262.158, 73.065
M4	4.16	N.F.	504.310	262.159	486.230, 468.289, 89.060
M5 (Terfenadine alcohol)	4.27	4.30	488.317	452.294	470.305, 262.159, 73.065
M6 (Terfenadine acid)	4.30	4.33	502.295	466.274	484.284, 262.159, 87.045

DMD Fast Forward. Published on April 28, 2014 as DOI: 10.1124/dmd.114.057430
This article has not been copyedited and formatted. The final version may differ from this version.

M7	4.45	4.49	486.301	219.138	468.289
M8	4.47	4.51	500.280	233.117	482.270
M9	4.51	N.F.	568.283	532.261	550.271, 488.315, 470.305, 452.295, 262.159, 98.985
M10	4.74	N.F.	634.374	436.299	616.360, 454.310, 262.159, 57.071
M11	4.74	N.F.	566.267	201.127	548.256, 299.104, 98.985
Terfenadine	4.91	4.94	472.321	436.299	454.310, 262.158, 57.071
M12	5.43	N.F.	552.289	436.299	454.309, 262.158, 57.071

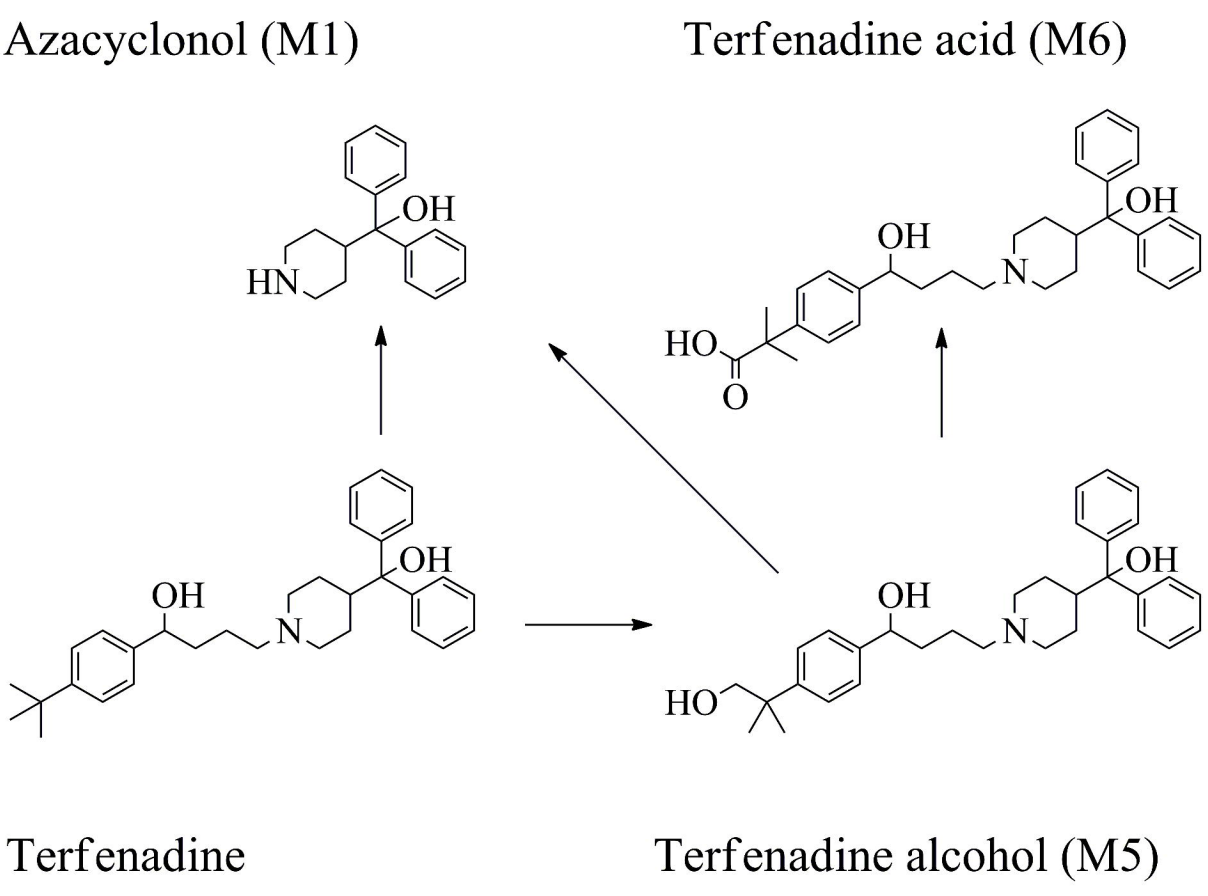
Azacyclonol (M1)
Terfenadine acid (M6)
Terfenadine
Terfenadine alcohol (M5)
OH
HN
HO
O
N

Figure 1

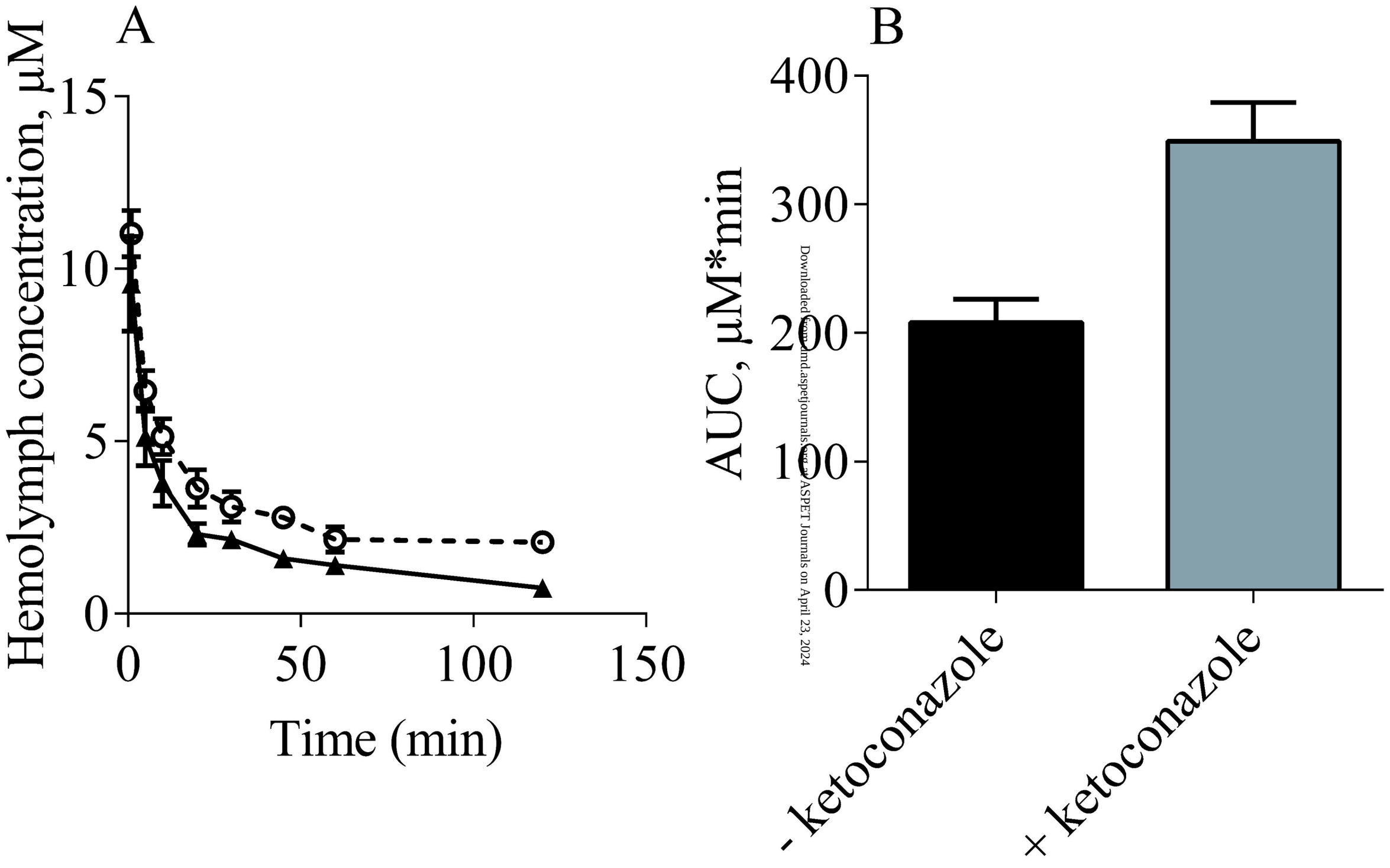

Figure 3

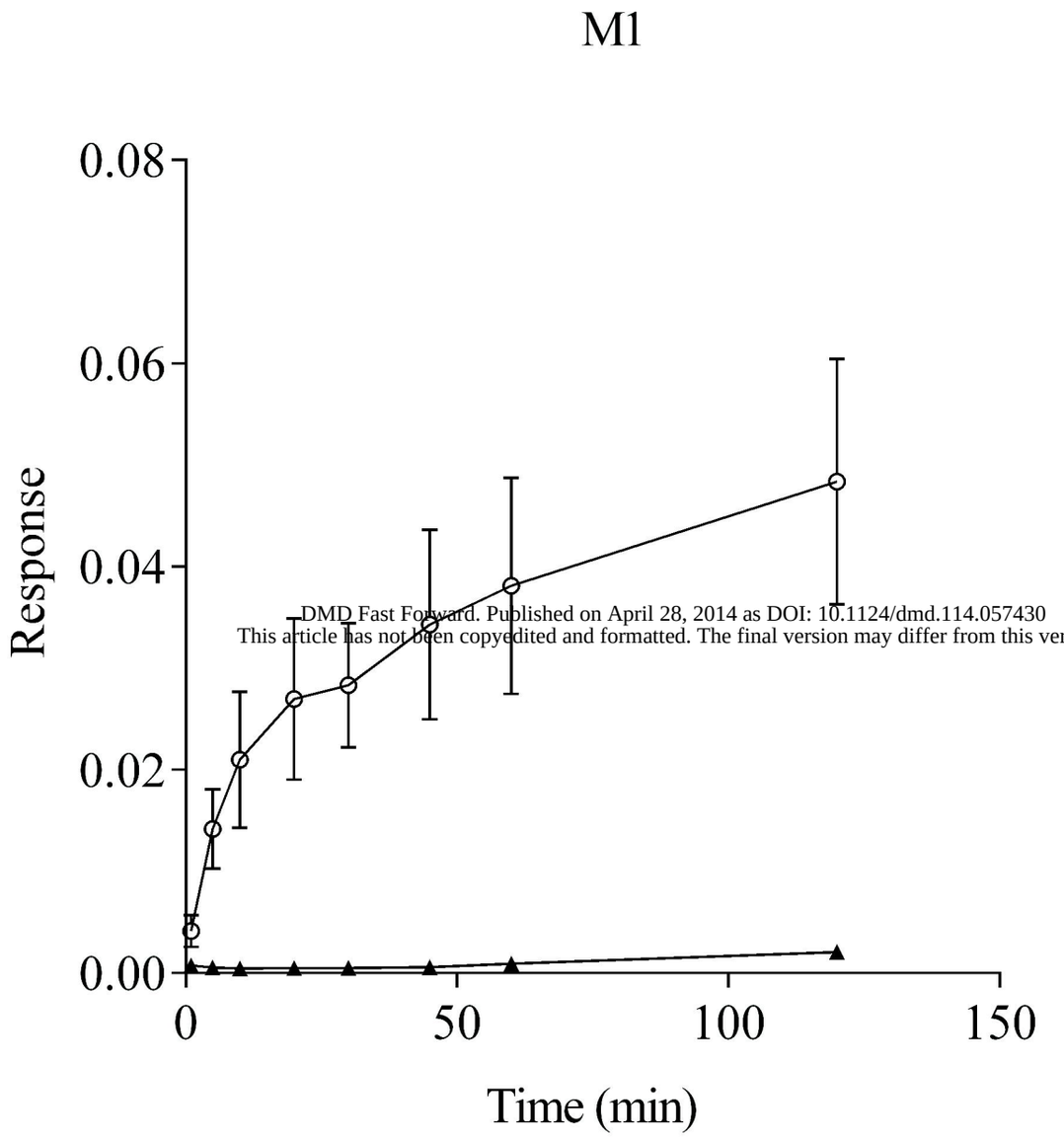

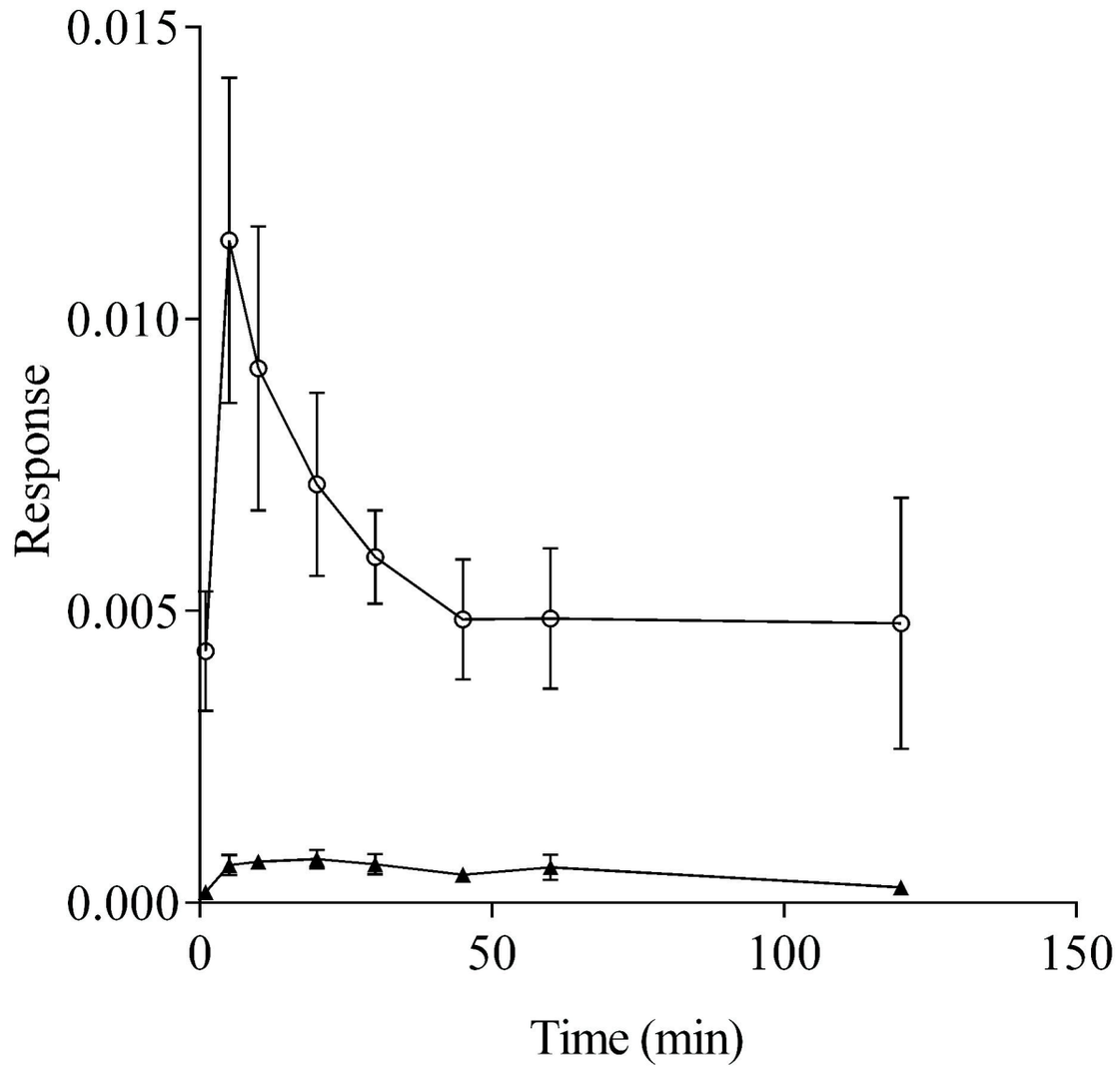

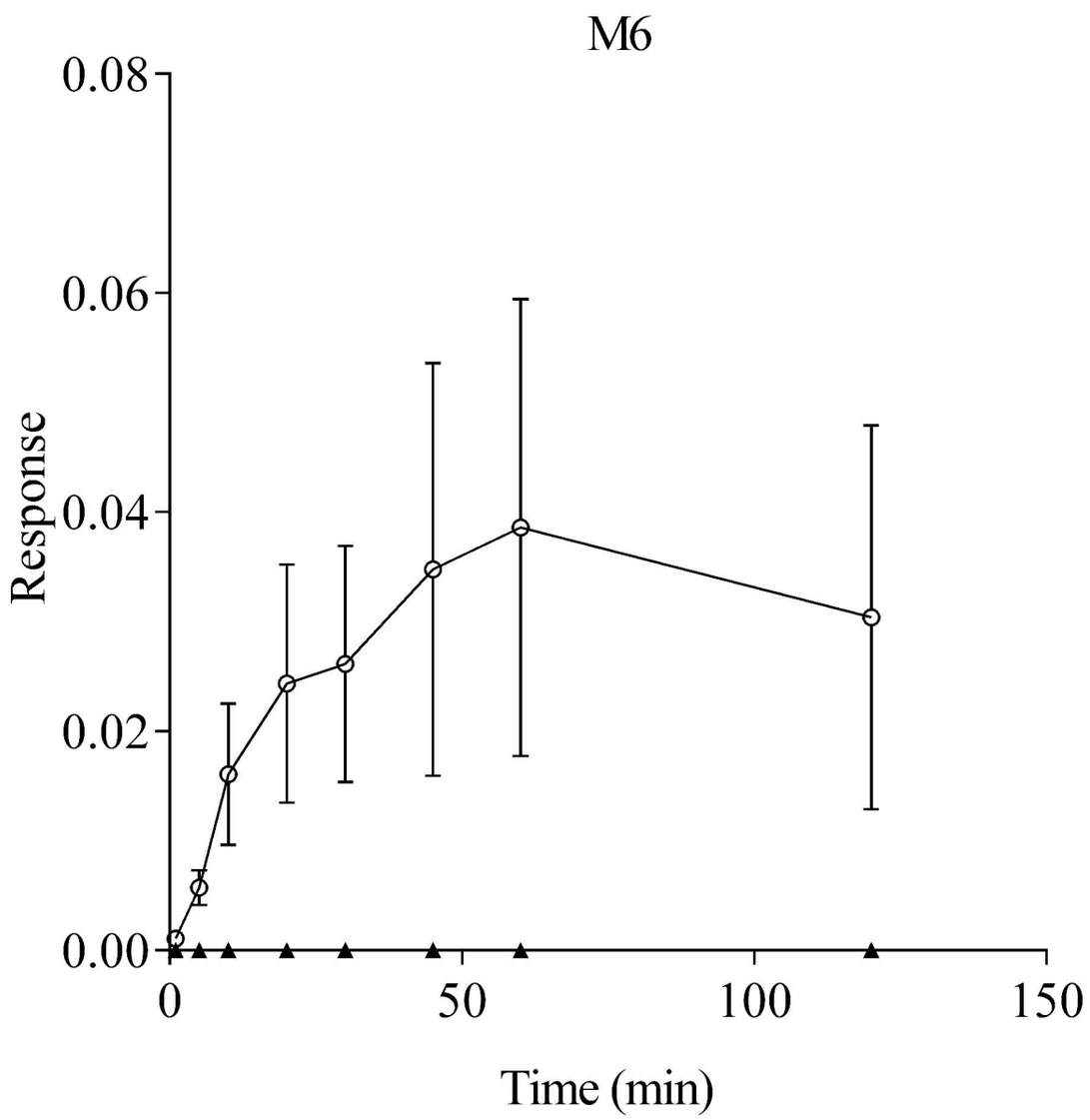

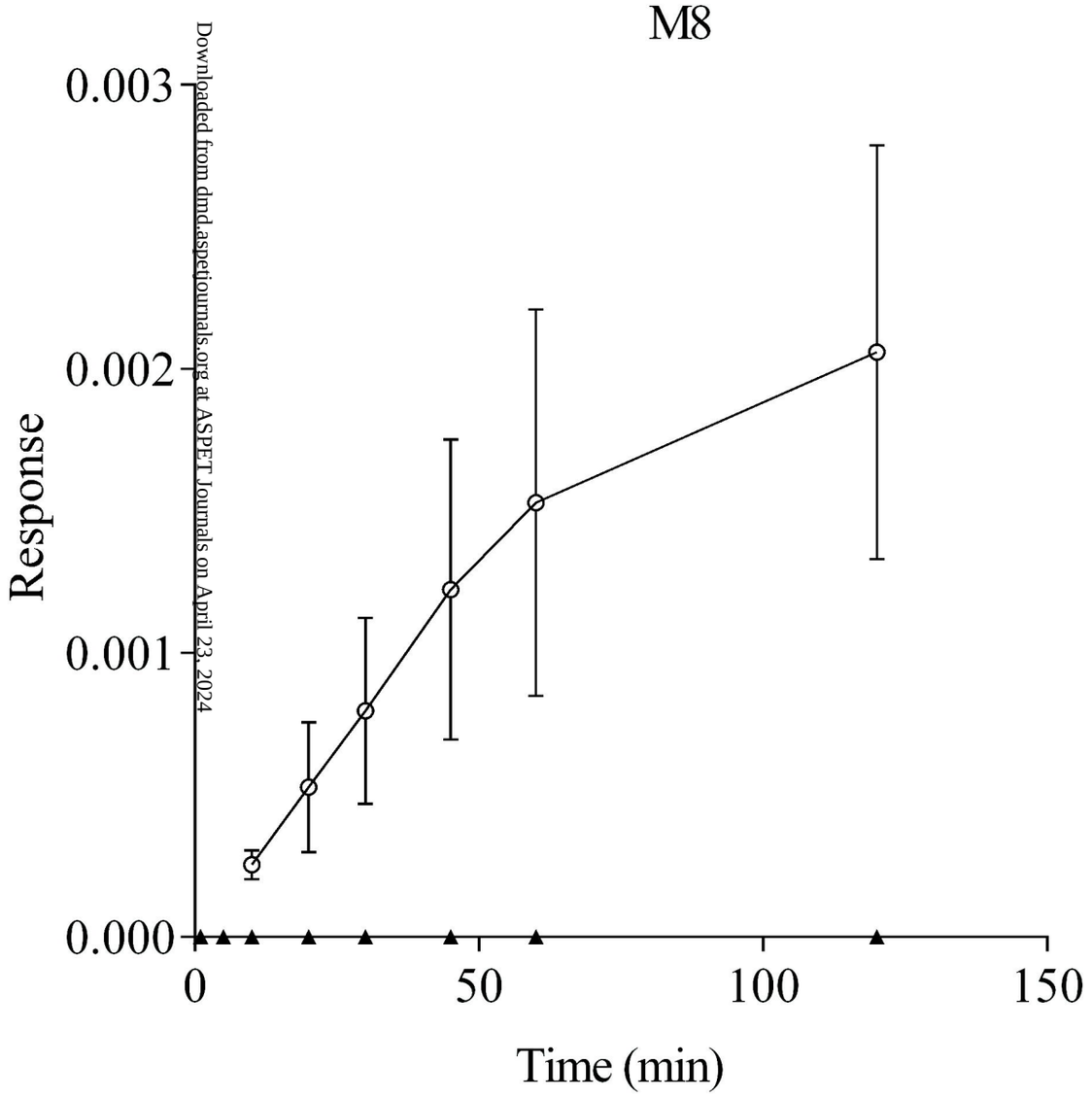

Figure 4

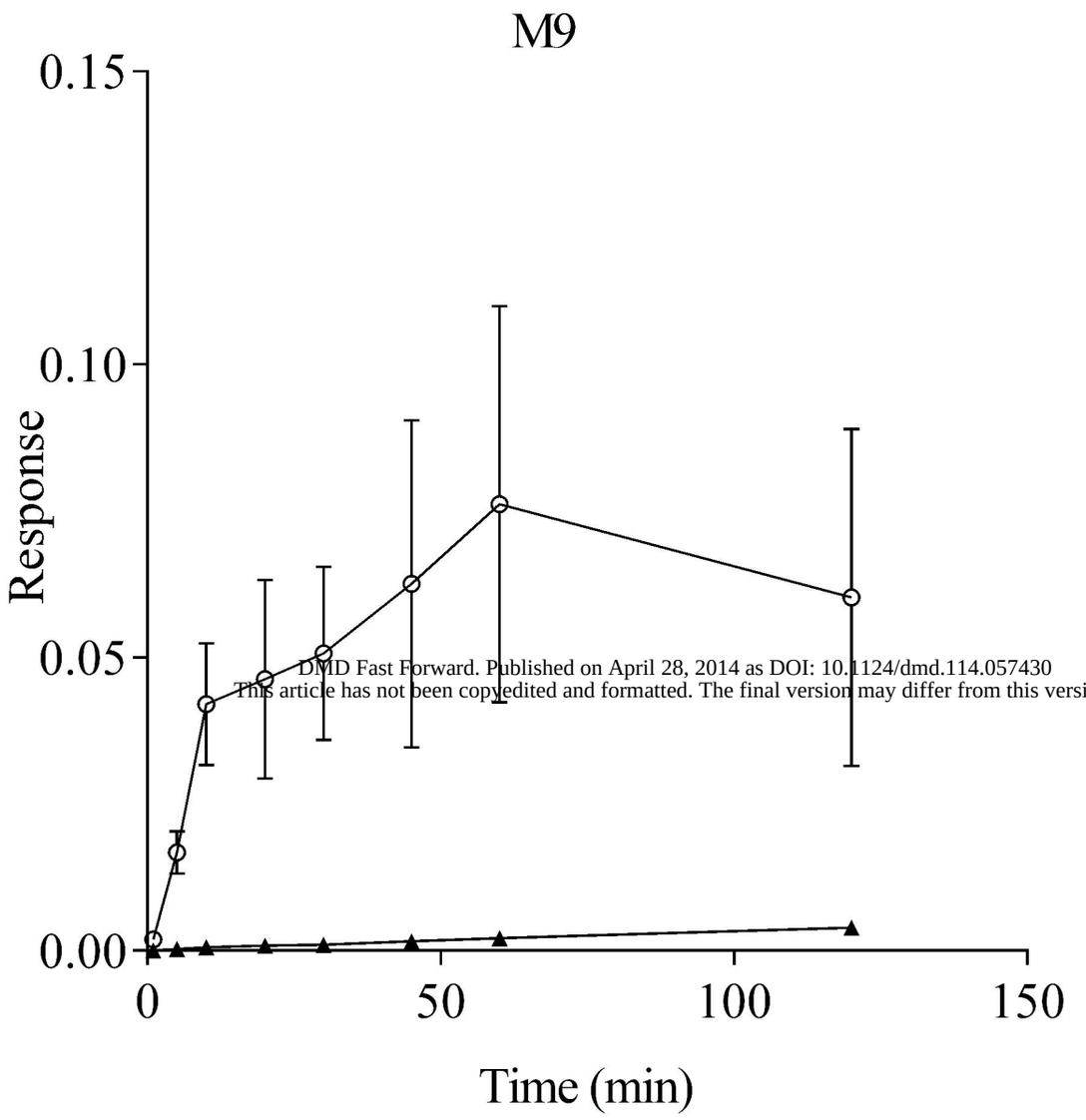

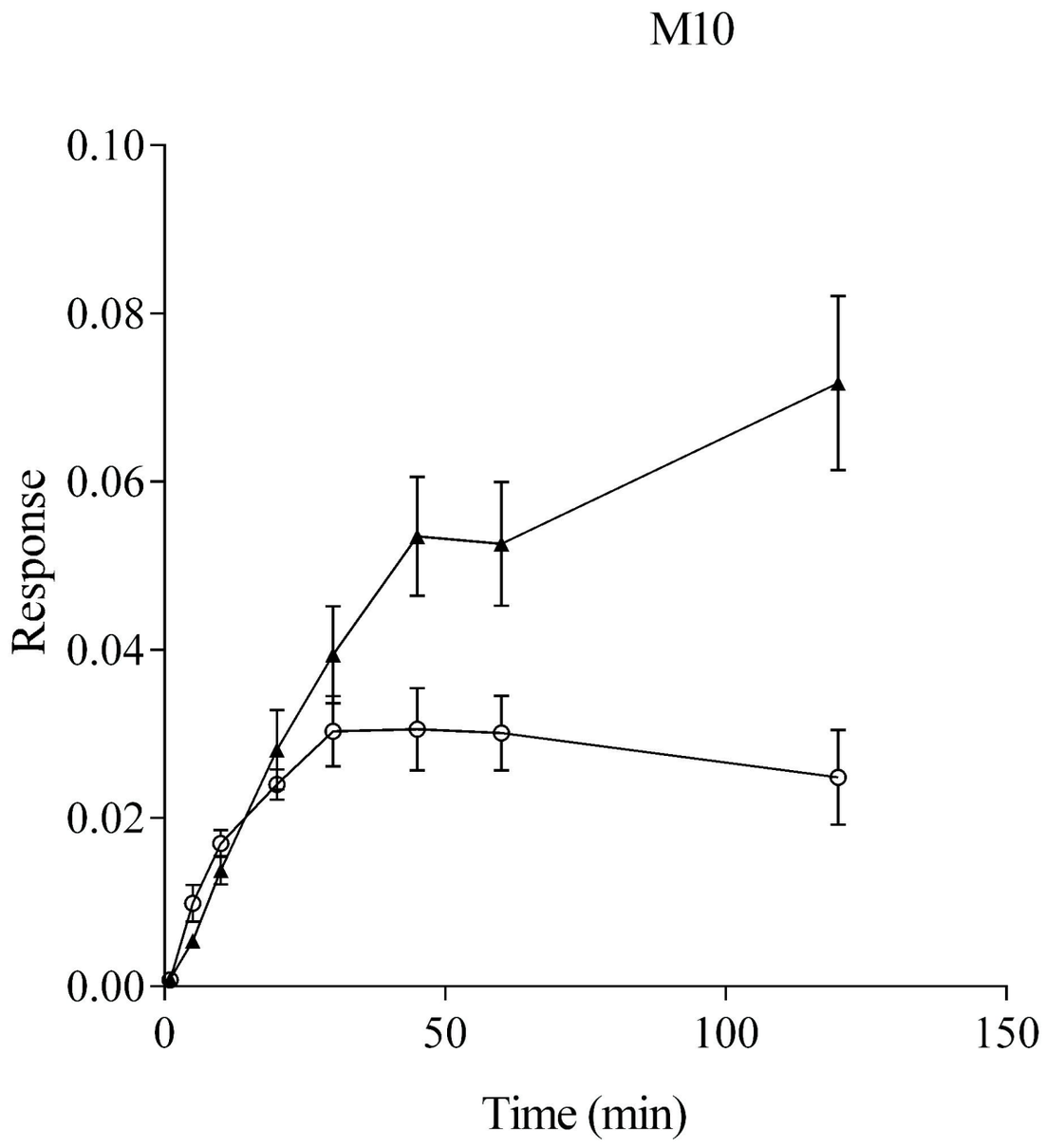

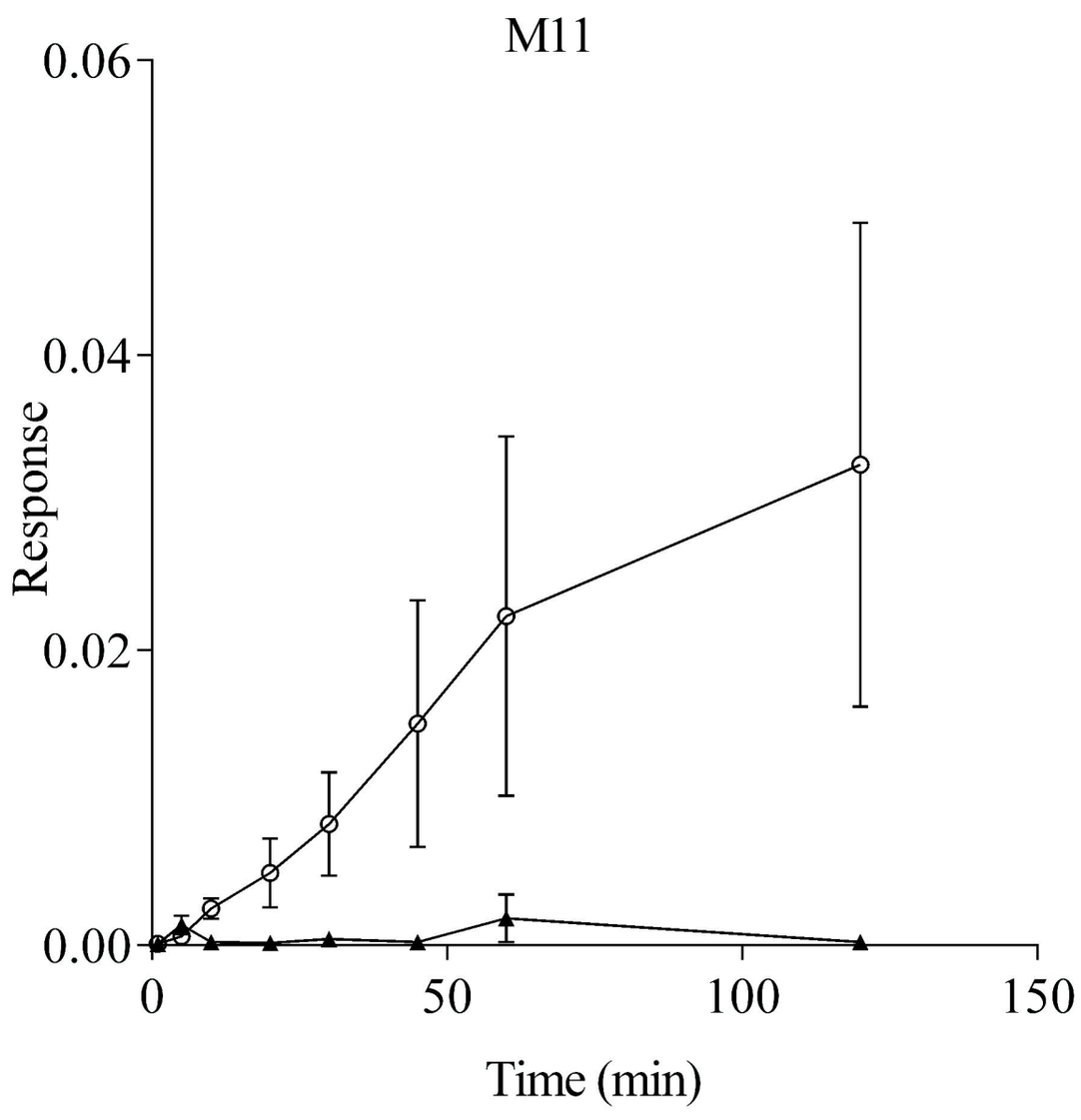

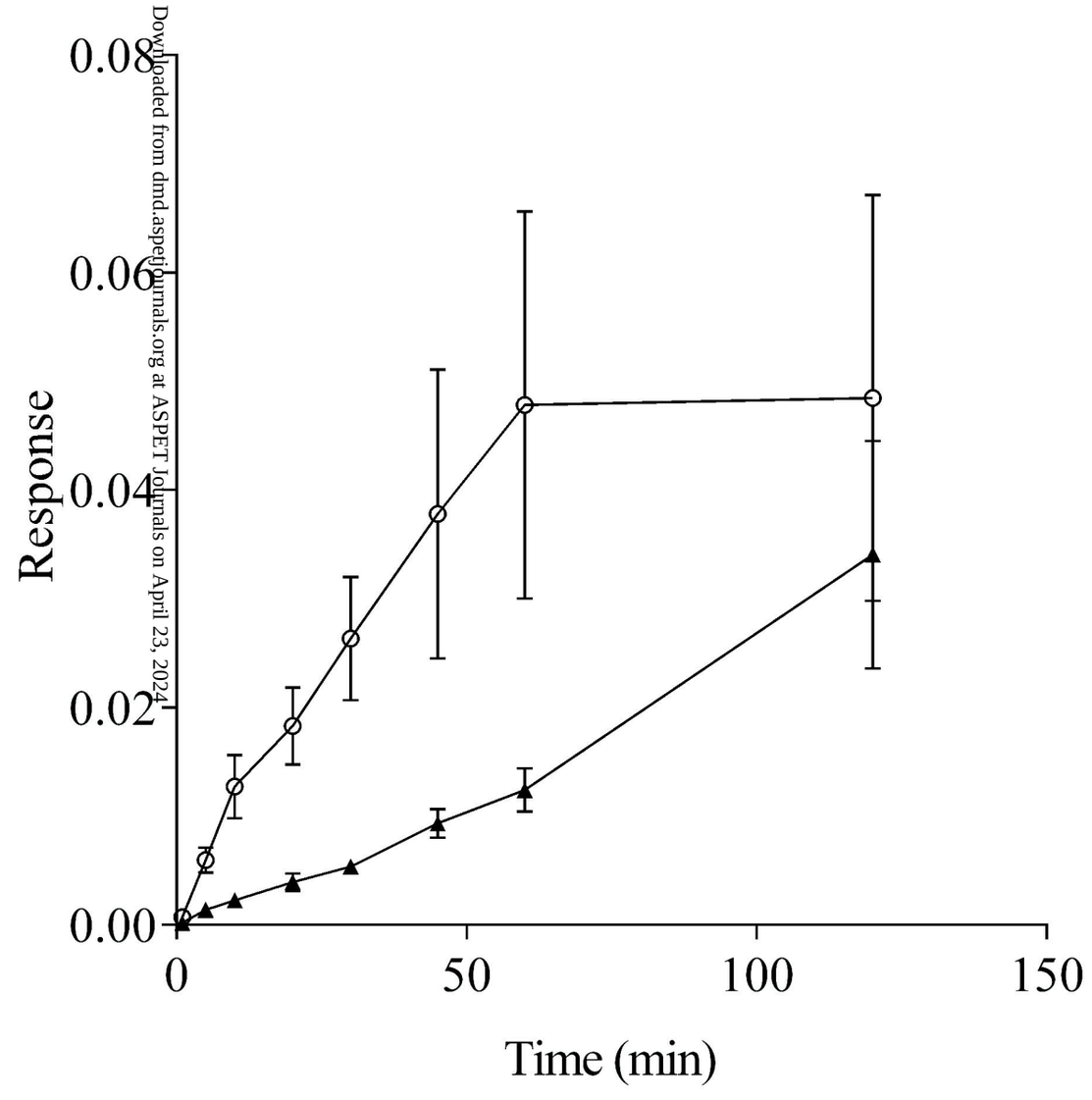

Figure 5

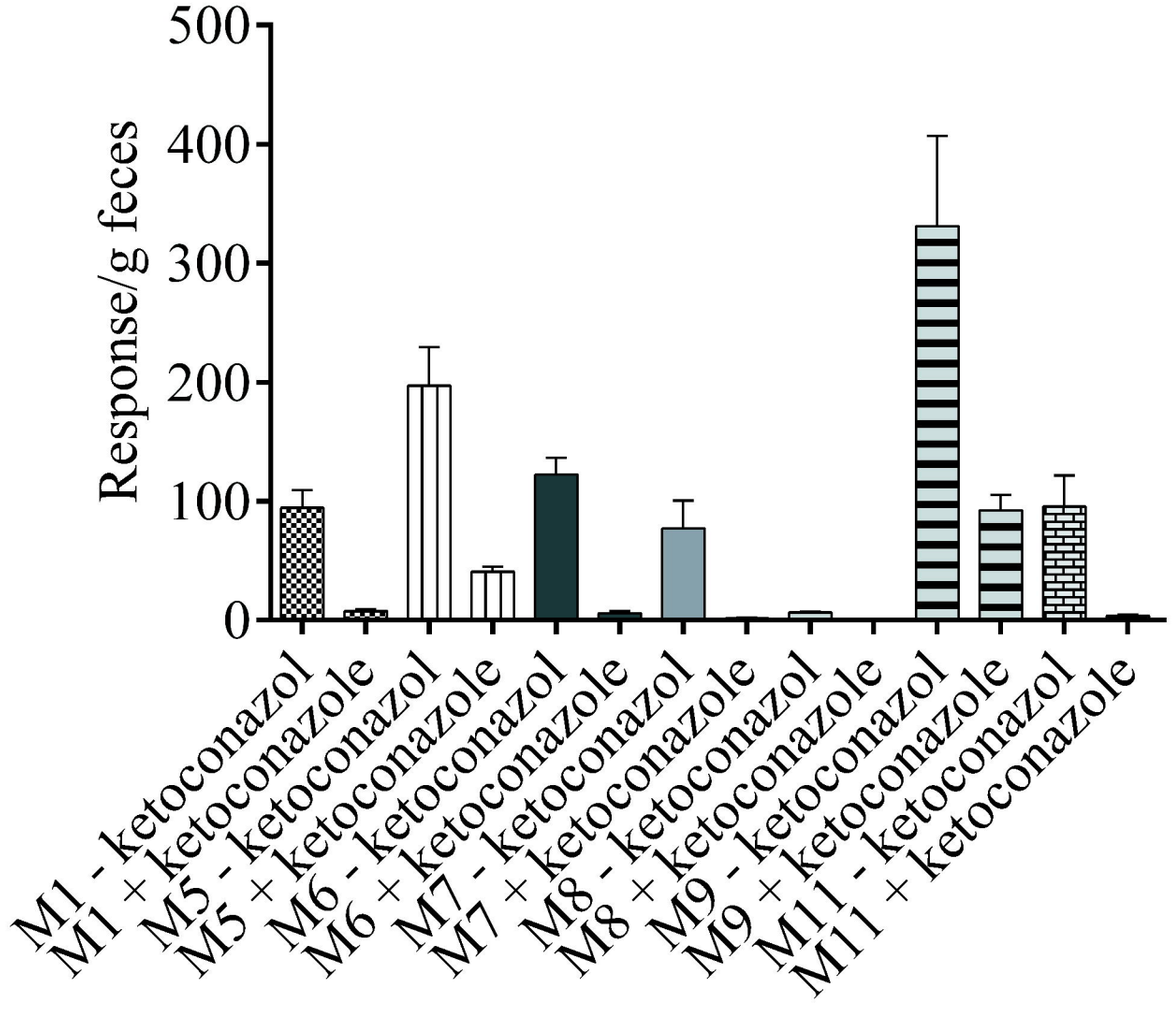

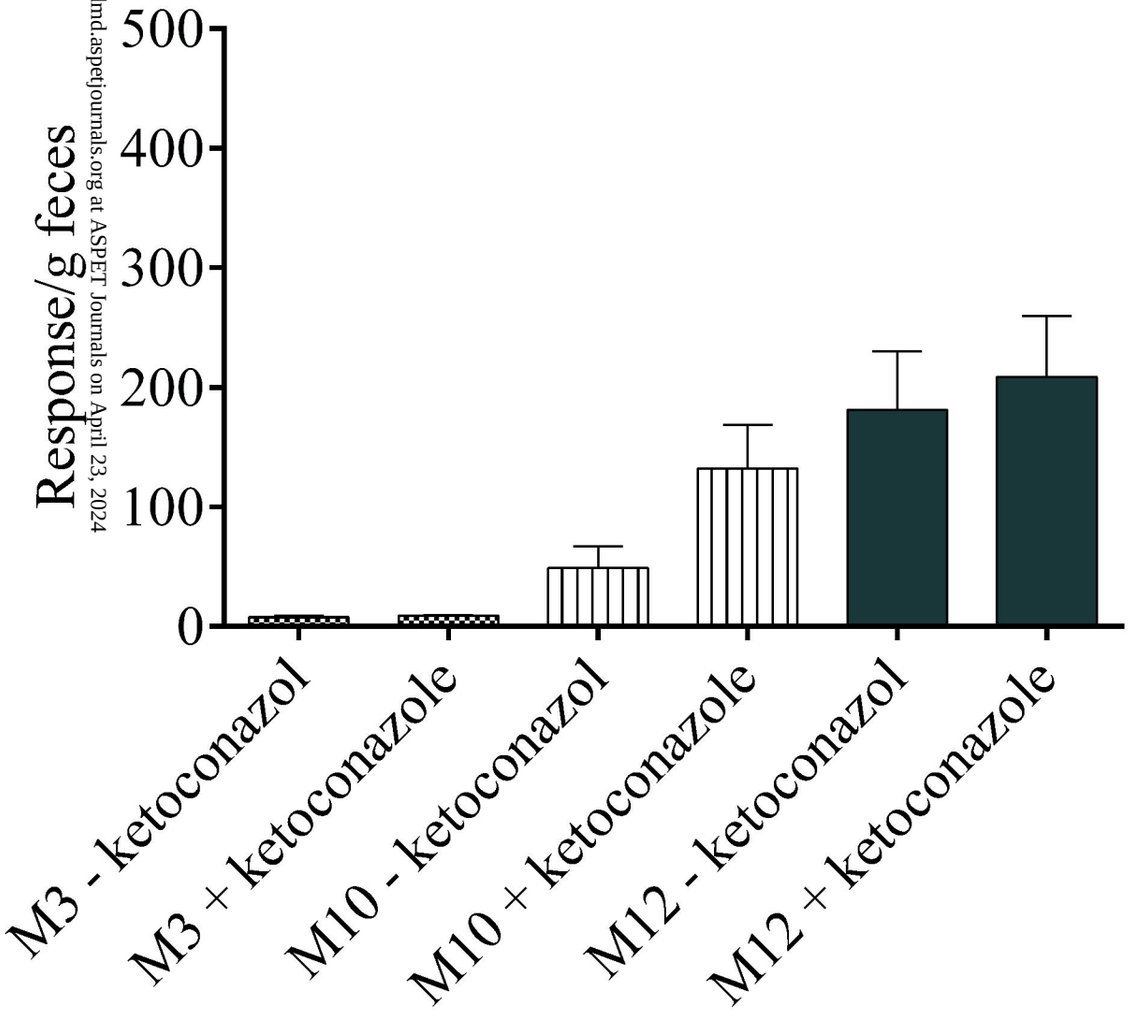

Figure 6

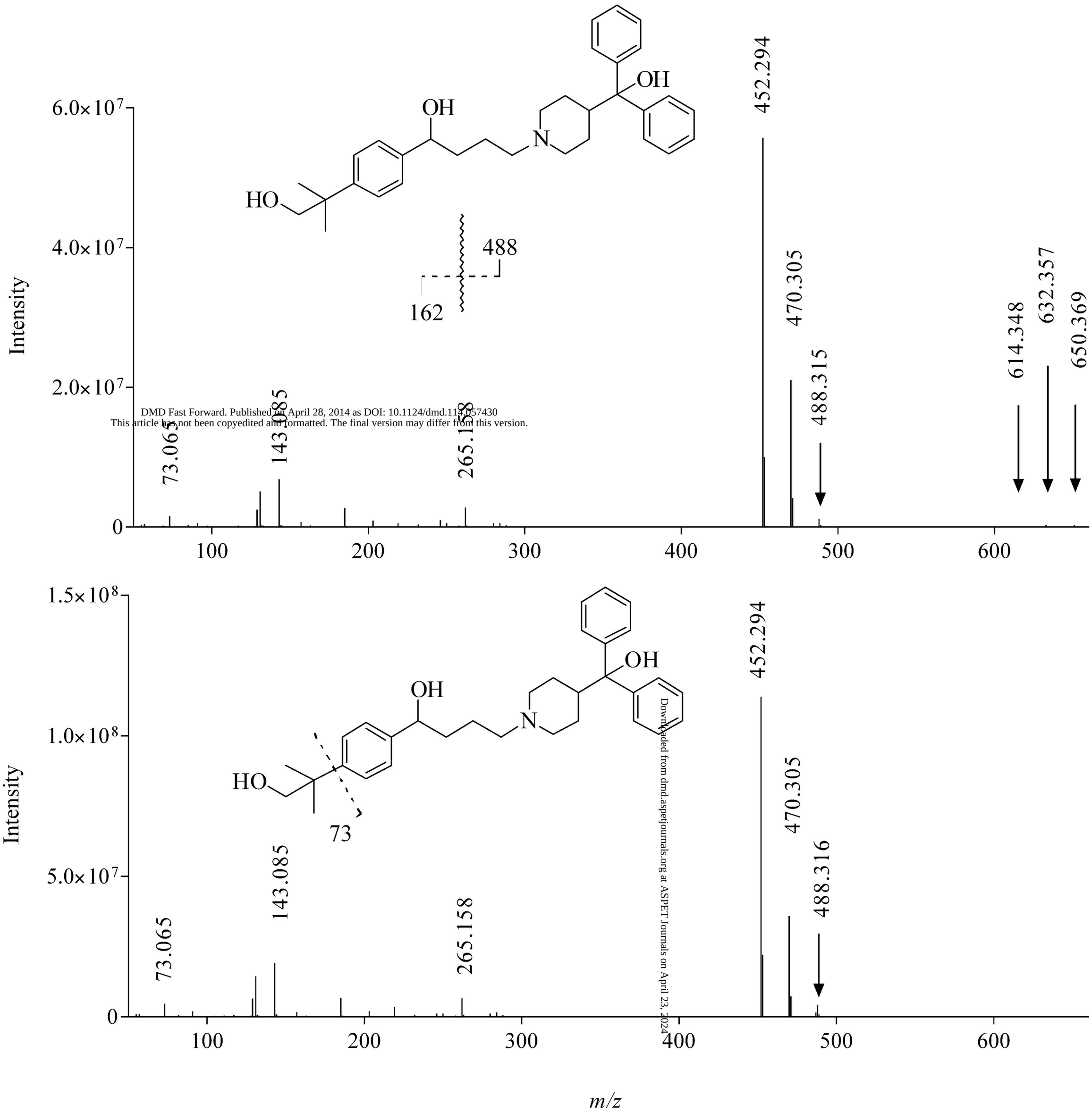

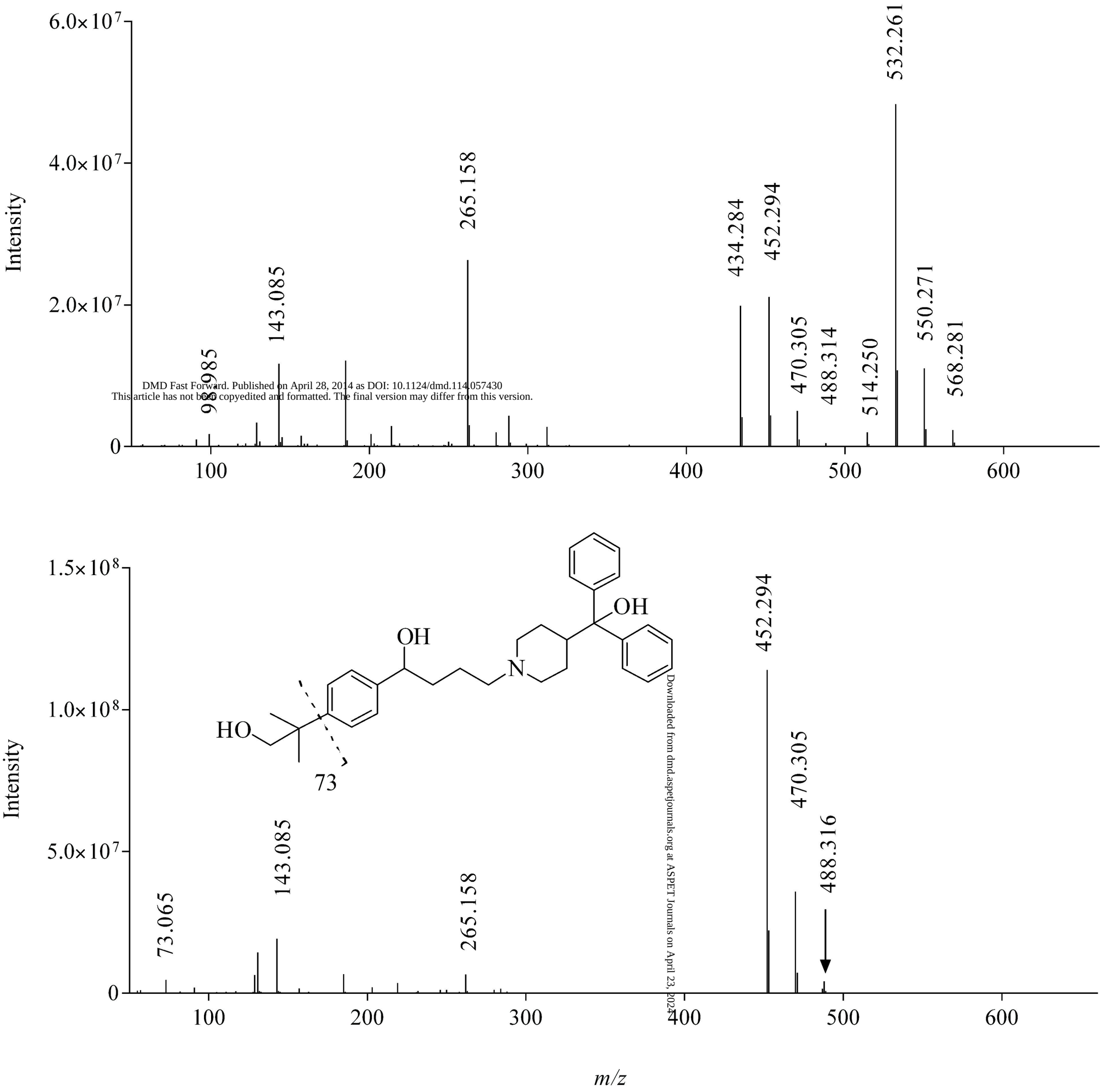

Figure 8

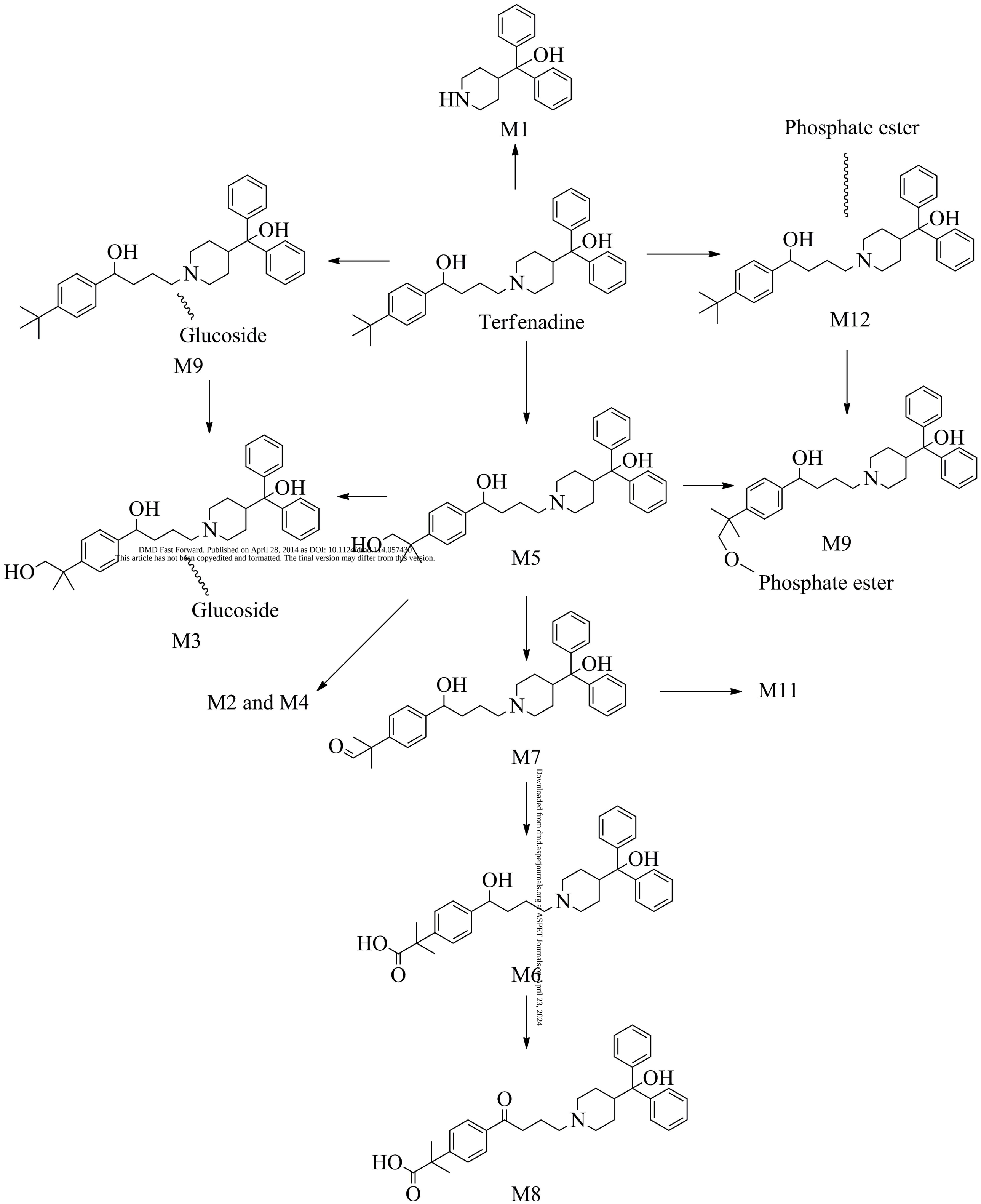

Figure 9